

Hadron Interactions

Arthur M. Moraes

*Department of Physics and Astronomy, Kelvin Building, University of Glasgow, G12 8QQ, Glasgow, UK
e-mail: a.moraes@physics.gla.ac.uk*

Abstract

Most of our information about the structure and properties of sub-atomic particles is based on the analysis of high-energy scattering data. Describing the dynamics of particle interactions, the Standard Model is currently the accepted theoretical framework of particle physics. In this paper, starting with a brief account of the history of particle physics, we review some aspects of the Standard Model which are used to describe high-energy hadron interactions.

1 Introduction

The 19th century saw the establishment of atoms as the basic elementary components from which chemical compounds, or molecules, are constructed. It can also be said that the 19th century witnessed the birth of particle physics. In 1897, while researching cathode rays, J. J. Thomson discovered the first elementary particle: the electron [1, 2].

At the start of the 20th century, E. Rutherford demonstrated that atoms consist of a tiny, positively charged and extremely dense nucleus which is surrounded by electrons [3]. By the early 1930s, J. Chadwick had discovered the neutron [4] and the quantum theory of the atomic structure had been developed. Atoms were shown to have a structure of bound states of negatively charged electrons and a positive nucleus held together by the electromagnetic forces due to the exchange of virtual photons.

It soon became apparent, however, that the structure of nature was more complicated. In the same year Chadwick presented his results proving the existence of neutrons, C. D. Anderson began his exploration of fundamental particles that are not found ordinarily in nature. Some months later Anderson would discover the positron, the first antimatter particle [5]. Still in the 1930s, observations of the decay of atomic nuclei indicated the presence of “mysterious” particles with little, or no mass, and no electric charge called neutrinos. The discoveries of positrons and neutrinos are just two examples of a series of particle discoveries, including the discovery of muons [6] and pions [7], which happened in the middle part of the 20th century and severely questioned the established theoretical description of the sub-atomic world [1].

A theory describing atomic nuclei as composites of varying numbers of protons and neutrons bound by the nuclear, or strong, interaction force stemming from the exchange of mesons was constructed during the 1930s and 1940s. However, as experiments involving the scattering of these supposedly elementary particles at high energies produced very large numbers of other, similar, strongly interacting particles, physicists were forced to recognise that protons and

neutrons were not structureless elementary particles, but simply the lightest members of a family of particles called ‘baryons’. Baryons and mesons are subject to the strong interaction and are grouped in a category of particles called ‘hadrons’ [8].

Already in the early 1960s the suggestion had been made that hadrons could conveniently be regarded as composites of more basic objects called ‘quarks’ [9]. At that time many physicists regarded these quarks as little more than a convenient mathematical device with which to model the properties of hadrons, since after all free quarks were not seen. However, it was not too surprising that when experiments to probe the structure of the proton by scattering electrons began at Stanford in the late 1960s it was revealed that protons did indeed contain point-like constituents. Later it would be shown that protons, and indeed all hadrons, are made of partons, i.e. quarks and gluons.

This probing of the constitution of matter has been made possible by the development of accelerators of increased energy and detectors capable of doing very precise measurements. A particle beam of momentum p has an associated wavelength given by

$$\lambda = \frac{h}{p}. \quad (1)$$

According to Heisenberg’s uncertainty principle, this determines the best spatial resolution which a beam of momentum p can provide. Thus, in order to probe the sub-atomic or partonic structure of a proton, one requires particle beam of at least 10 GeV.

A continuous evolution on accelerators and detection techniques has allowed particle physics to reveal systematically the fundamental structure of the sub-atomic world. In 1995, the discovery of the top quark at Fermilab [10], completed the set of elementary particles and was the final piece in the story that had begun with Thomson nearly a century earlier.

The present state of our knowledge on elementary particles and their fundamental interactions is summarised in the Standard Model of particle physics, briefly reviewed in the section below. As we shall discuss in the following sections,

hadrons, which are made of more elementary objects (i.e. partons), interact at high-energy through the mediation of these elementary objects. Thus, the description of a hadron-hadron scatter at high-energy is the product of interactions between the elementary particles which constitute the scattered hadrons.

2 The Standard Model

The advent of the Standard Model (SM) and its remarkable success in describing most of the observed data in high-energy physics is certainly one of physics' greatest achievements of last century. The SM is well described in great detail in many textbooks [11], so will only be briefly discussed here.

Experimental evidence indicates that the universe is made of two kinds of fundamental particles, fermions and bosons, governed by four kinds of forces: the electromagnetic, weak, strong and gravitational forces. The SM provides a theoretical description of the electromagnetic, weak and strong interactions in terms of gauge theories.

According to the SM, fermions make up matter and the interactions between particles of matter are mediated by force carriers also known as gauge bosons. The fundamental particles and interactions described by the SM are presented below.

2.1 Leptons and Quarks

Elementary (or structureless) spin 1/2 fermions can be grouped into two categories: leptons and quarks.

Leptons exist as either charged or neutral particles. Carrying an electric charge of -1 (in units of the electron's charge), charged leptons are the electron (e), muon (μ) and tau (τ), in order of increasing mass. Associated with each charged lepton is a left-handed electrically neutral neutrino: ν_e , ν_μ and ν_τ . Electrons, muons and taus are subject to electromagnetic and weak interactions whereas neutrinos are sensitive only to the weak force.

Quarks carry a fractional electric charge of +2/3 for the up (u), charm (c) and top (t) quarks, and -1/3 for the down (d), strange (s) and bottom, or beauty, (b) quarks. To date no free quarks have been observed. They are confined within composite particles called hadrons, which may be either mesons or baryons. Mesons are quark-antiquark ($q\bar{q}$) bound states while baryons are three quark (qqq) bound states.

Quarks are subject to the strong, weak and electromagnetic interactions. Quarks also carry an additional charge, known as colour charge, which distinguishes them from leptons.

There are three colour charges and three corresponding anticolour charges. Each quark has one of the three colour charges and each antiquark has one of the three anticolour charges. Just as a mix of red, green, and blue light yields

white light, in a baryon a combination of "red," "green," and "blue" colour charges is colour neutral, and in an antibaryon "antired," "antigreen," and "antiblue" is also colour neutral. Mesons are colour neutral because they carry combinations such as "red" and "antired."

Leptons and quarks can be arranged in three generations, or families, organised by increasing mass as shown in table 1.

Table 1: Lepton and quark generations as described by the SM.

Leptons	$\begin{pmatrix} e \\ \nu_e \end{pmatrix}$	$\begin{pmatrix} \mu \\ \nu_\mu \end{pmatrix}$	$\begin{pmatrix} \tau \\ \nu_\tau \end{pmatrix}$
Quarks	$\begin{pmatrix} u \\ d \end{pmatrix}$	$\begin{pmatrix} c \\ s \end{pmatrix}$	$\begin{pmatrix} t \\ b \end{pmatrix}$
Generations of matter	1st	2nd	3rd

2.2 Fundamental Interactions

Leptons and quarks are subject to four kinds of forces: electromagnetic, weak, strong and gravity.

One of the simplest interactions is electromagnetism, which is described by quantum electrodynamics (QED). This interaction affects all charged particles and manifests itself in the effects of electricity and magnetism. It binds negative electrons to the positive nuclei in atoms and underlines interactions between atoms giving rise to molecules.

Weak interactions are the only processes in which a quark can change to another type of quark, or a lepton to another lepton. They are responsible for the fact that all the more massive quarks and leptons decay to produce lighter quarks and leptons. That is why stable matter around us contains only electrons and the lightest two quark types (up and down). The weak force leads to the decay of neutrons, accounting for the production of many natural occurrences of radioactivity, and allows the conversion of a proton into a neutron, explaining the hydrogen burning in the centre of stars.

Eventually it was discovered that at very short distances (about 10^{-18} m) the strength of the weak interaction is comparable to that of the electromagnetic. On the other hand, at thirty times that distance (3×10^{-17} m) the strength of the weak interaction is 1/10,000th that of the electromagnetic interaction. At distances typical for quarks in a proton or neutron (10^{-15} m) the force is even tinier.

The strong force holds quarks together within protons, neutrons and other hadrons. It also guarantees that protons are held together inside the nucleus and not moved apart by repulsive electrical forces. This is because, within the nucleus, the strong force is about 100 times stronger than the

electromagnetic one. Strong interactions are described by quantum chromodynamics (QCD).

Gravity is perhaps the most familiar of the fundamental forces, but has no measurable effects on the scale of particle interactions and is not included in the SM. Gravity will not be further discussed in this dissertation.

The SM is made up from three gauge theories, which means that it is built up from three gauge symmetries. The SM gauge group is the product group $SU(3)_C \times SU(2)_L \times U(1)_Y$, with the $SU(3)_C$, $SU(2)_L$ and $U(1)_Y$ component groups associated with the colour, weak isospin and hypercharge symmetries. The corresponding gauge bosons are the massless gluons of QCD, the massive W^+ , W^- and Z bosons of the weak interaction and the massless photon of the electromagnetism.

Table 2 summarises the fundamental interactions described by the SM, their gauge bosons or force carriers, effective range and the particles which are sensitive to them.

[h]

Table 2: Fundamental interactions described by the SM.

Interaction	Gauge Boson	Range (m)	Sensitive Particles
Electromagnetic	Photon (γ)	∞	charged particles
Weak	W^\pm, Z	$< 10^{-16}$	leptons, quarks
Strong	Gluon (g)	$\sim 10^{-15}$	quarks

The fact that W and Z bosons are observed to be massive (with measured masses of 80.4 and 91.2 GeV respectively [15]) poses a severe problem to the gauge theory which describes electroweak interactions. In an unbroken gauge theory the gauge bosons must be massless. Massive W and Z bosons indicate that the symmetry of the electroweak gauge theory is somehow broken.

An elegant solution to this problem is provided by the Higgs mechanism. Through the Higgs mechanism, the W and Z bosons acquire mass via the spontaneous symmetry breaking of an additional field - the Higgs field, which has a non-zero vacuum expectation value. The gauge symmetry is then still present, but hidden, and the mass terms of W and Z bosons do not destroy it. This mechanism produces an additional spin 0 particle, the so-called ‘‘Higgs boson’’, and can also be used to explain how other fundamental particles acquire mass preserving gauge invariance.

2.3 The Standard Model: an Incomplete Theory

The SM has had many remarkable successes. The unification of electromagnetism and the weak force into a single electroweak theory, the predictions of W and Z bosons,

successfully confirmed by UA1 and UA2 experiments at the CERN’s SPS [12, 13]. The prediction of the existence of the top quark, later found by CDF and D0 experiments [10] at the Fermilab’s Tevatron, as well as the predictions of the top quark mass based on e^+e^- data, testing the electroweak sector at the level of radiative corrections, also figure as some of the most prominent examples of the predictive power of the SM.

Many other experiments performed at the Large Electron Positron Collider (LEP), Stanford Linear Accelerator Center (SLAC) and several other laboratories, have tested and verified weakly interacting predictions made by the SM to unprecedented precisions. Furthermore, a number of predictions made by perturbative QCD have also been confirmed in deep inelastic scattering and in jet physics.

However, despite its tremendous successes, the SM remains theoretically unsatisfactory. One of the reasons for this is that the SM has 19 independent parameters. These include 3 gauge couplings, 9 fermion masses (6 quarks and 3 leptons), 3 weak mixing angles, 2 parameters of the Higgs sector, 1 phase in the Cabibbo-Kobayashi-Maskawa (CKM) matrix and the vacuum parameter of QCD. These parameters have to be set by hand and we have no real understanding of why they take the values that are observed.

The SM also fails to explain why three generations of fermions are observed and what is the origin of particle masses. It does not explain the origin of the asymmetry between matter and anti-matter in the universe (CP-violation), does not include gravity and does not provide a dark matter candidate.

The development of models that go beyond the SM, such as Supersymmetry (SUSY) or Grand Unified Theories (GUTs), would be expected to provide answers to such questions.

3 The Strong Interaction

The strong interaction is the result of the exchange of massless gluons between coloured quarks.

The colour property of quarks was initially introduced by the quark model to explain how resonances such as the Δ^{++} , Δ^- and Ω^- which consist of three quarks with the same flavour ($\Delta^{++} = uuu$, $\Delta^- = ddd$ and $\Omega^- = sss$) and parallel spins (Δ^{++} , Δ^- and Ω^- are spin-3/2 particles), do not violate the exclusion principle. Since quarks are fermions and should have a wave-function which is antisymmetric under the interchange of the quantum numbers of any two fermions, only by postulating that quarks, as well as flavour also carry one of three colours (red, green or blue), Δ^{++} and similar resonances could be explained [8, 11].

A quark field is therefore described by specifying its flavour and colour contents and can be written as q_f^i , where

f is the flavour index (u, d, s, c, b or t) and $i = 1, 2$ or 3 (alternatively R, G or B for red, green and blue), is the colour index.

The strong interactions are invariant under colour SU(3) transformations. As previously mentioned, QCD is the gauge theory which describes the strong interactions. According to this theory, quarks transform as a triplet representation of the group SU(3). Furthermore, it is also assumed that hadrons are singlets of this SU(3) group or, in other words, described as colourless states composed of three quarks (baryons) or of a quark and an anti-quark (mesons).

QCD introduces eight gauge bosons in order to preserve gauge invariance. These correspond to eight massless gluons and are taken to be the force carriers which mediate strong interactions in a similar way that photons are the carriers which mediate the electromagnetic interactions.

3.1 QED and QCD Couplings

The fact that gluons are massless suggests that the potential associated to strong interactions might be expected to fall with the distance r as $1/r$, as in QED. However, the QCD potential actually behaves very differently of its QED counterpart at large distances.

In quantum field theories any charge is shielded by a cloud of polarised charges. The lowest order QED process gives rise to the Coulomb interaction potential $V(r)=\alpha/r$ which is proportional to α , where $\alpha = e^2/4\pi\hbar c \simeq 1/137$. Higher order QED contributions involve more couplings and hence are smaller by further powers of α , often being neglected. However, it is important to point out that the physical coupling increases with the transferred momentum Q^2 , where $Q^2 \equiv -q^2$ and q is the four-momentum of the virtual photon. This is due to vacuum polarisation effects that shield the bare electromagnetic charge.

For $Q^2 \gg \mu^2$, where μ is the arbitrary normalisation point at which α is measured, $\alpha(Q^2)$ is given by [11]:

$$\alpha(Q^2) \simeq \frac{\alpha(\mu^2)}{1 - [\alpha(\mu^2)/3\pi]\ln(Q^2/\mu^2)}. \quad (2)$$

Notice that the QED coupling, $\alpha(Q^2)$, is not really a constant at all and varies, or “runs”, with Q^2 .

According to the uncertainty principle, Q^2 is canonically conjugated to the wavelength with which the virtual photon probes the electric charge. This means that as Q^2 increases the corresponding wavelength of the virtual photon decreases and the photon sees more and more of the bare charge. Because of this effect, also known as charge screening, the charge one measures depend on the distance or wavelength with which one is probing the charge itself.

At some very large, though not necessarily infinite Q^2 , the coupling $\alpha(Q^2) \rightarrow \infty$, and the bare charge is said to be

ultraviolet divergent. On the other hand, at the infrared region of experimental QED, the Q^2 dependence of $\alpha(Q^2)$ is practically undetectable.

In QCD the strong coupling, $\alpha_s(Q^2)$, dependence on Q^2 is the opposite to the one seen for the QED coupling. Gluons carry colour and hence couple to each other, which does not happen in QED since photons do not carry electromagnetic charge. QCD is therefore said to be a non-Abelian gauge theory, i.e. a field theory in which the field quanta (gluons) may interact directly coupling to each other.

The lowest-order diagram of a $q\bar{q}$ interaction involving a single gluon exchange is shown in Figure 1(a). The diagrams in Figures 1(b) and (c) are the lowest-order corrections to the quark-gluon coupling.

The effect of higher order diagrams like the ones shown in Figures 1(b) and (c) gives

$$\alpha_s(Q^2) \simeq \frac{1}{(b_0/4\pi) \ln(Q^2/\Lambda^2)}, \quad (3)$$

where $\Lambda^2 \equiv \mu^2 \exp(-4\pi/\alpha_s b_0)$, μ^2 is the value of Q^2 at which α_s is measured and $b_0 \equiv \frac{11}{3}N_c - \frac{2}{3}N_f$. N_c is the number of colours and N_f is the number of quark flavours [8].

The N_c term stems from the gluon loop shown in Figure 1(c). Gluon loops are formed because gluons carry colour and hence couple to each other. No similar contribution is found in QED. The quark loop shown in Figure 1(b) is responsible for the N_f term, and in this case, similar contributions are found in QED.

With three colours ($N_c = 3$) and six flavours ($N_f = 6$) $b_0 = 7$ and the sign in the denominator of equation (3) is opposite to that in (2). This implies that as $Q^2 \rightarrow \infty$ the strong coupling $\alpha_s(Q^2) \rightarrow 0$ and means that quarks and gluons appear like almost free particles when probed at very high Q^2 or short distances. This asymptotic freedom allows perturbation theory to be applied to theoretical QCD calculations and is one of the essential ingredients of the parton approach to the structure of hadrons as well as to the description of deep inelastic scattering data [8].

Equation (3) also indicates that $\alpha_s(Q^2) \rightarrow \infty$ when $Q^2 \rightarrow \Lambda^2$. As a consequence, perturbation theory breaks down at small Q^2 , or in other words, as the separation between the q and \bar{q} increases their colour interaction becomes stronger and the perturbation theory breaks down as $r \rightarrow 1/\Lambda$. This phenomenon is called infrared slavery and is believed to be the origin of the quark confinement into colourless hadrons, explaining why free quarks are not observed.

The confinement range of quarks and anti-quarks inside a hadron is of the order $\hbar c/\Lambda$. Based on the fact that hadrons have a size $\sim 1\text{fm}$, Λ_{QCD} is defined as

$$\Lambda_{\text{QCD}} \simeq 0.2\text{GeV}. \quad (4)$$

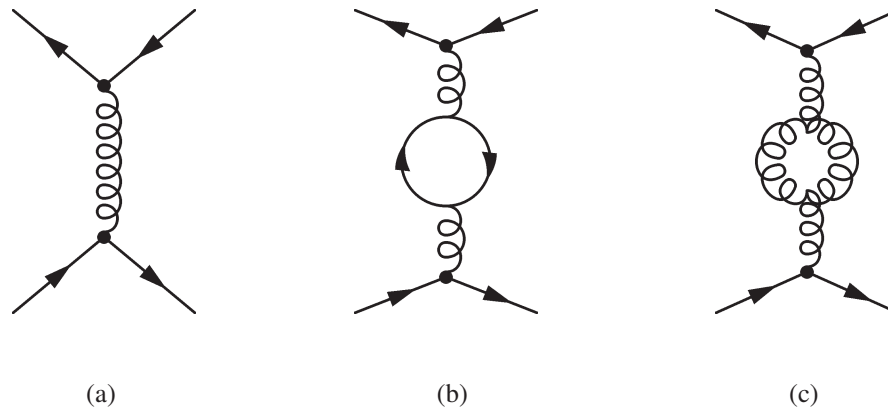


Figure 1: (a) Lowest-order $q\bar{q}$ interaction; (b) and (c) lowest-order corrections to the quark-gluon coupling.

4 Hadron Scattering

Hadrons are clusters of confined partons (quarks, anti-quarks and gluons) which may be either mesons ($q\bar{q}$) or baryons (qqq). Although each hadron is an overall colourless cluster of partons, within it there will be a distribution of colour charges. As two hadrons, A and B, approach each other, the potential associated to the strong force induces a redistribution of the colour charge within each of the colliding hadrons, just like the atom's electron distribution is induced (or polarised) by a passing electrically charged particle.

Based on the experimental result of a high-energy hadron collision, high-energy hadron scatterings can be divided into two categories: elastic and inelastic scatterings.

In elastic scatterings, both colliding hadrons retain their integrity and are not broken up to form new hadrons. This is only likely if there is very little momentum transferred by the colour polarisation force. Two hadrons, A and B, undergoing an elastic scattering are represented as $AB \rightarrow AB$.

Inelastic scatterings are characterised by the break up of one or both colliding hadrons. They are sub-divided into diffractive (single and double diffraction) and non-diffractive processes [14]. A typical inelastic scattering may be viewed as the schematic picture shown in Figure 2

In inelastic scatterings, one or both of the hadrons may be rather little affected by the interaction. However, because of the excitation their internal partonic structure may be rearranged forming new colourless hadrons, which are called fragments. Fragments carry a significant fraction of the momentum of their "mother" particle and manifest themselves as spreads or jets of a few highly energetic particles in the forward or backward (or both) directions.

Processes where only one of the incoming hadrons is excited to the point of fragmenting itself into new hadrons are named single diffractive scatterings. In these processes, the centre-of-mass energy is much larger than the momentum transferred by the field excitation. Single diffractive events result in jets of particles [8] either in the forward or back-

ward directions with an empty central region (i.e. the angular region which is transverse to the colliding beam) and can be represented as $AB \rightarrow AX$ or $AB \rightarrow XB$, depending on whether A or B undergoes a single diffraction, with X being anything else produced by the break up of A and/or B in the final state.

Scatterings where both hadrons are excited by the colour field, later fragmenting into hadrons which make up jets of particles in both forward and backward regions, are named double diffractive. These processes are represented as $AB \rightarrow X_1 + X_2$.

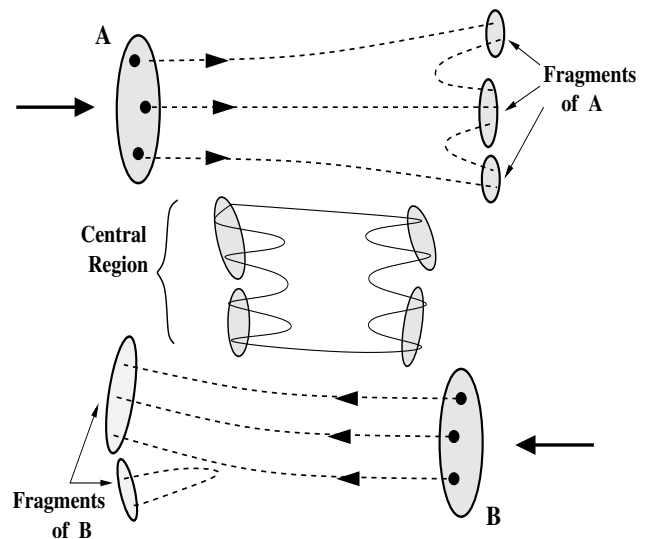


Figure 2: Schematic view of an inelastic hadron scattering.

The remaining contribution to inelastic events is labelled non-diffractive and is represented by the generic process $AB \rightarrow X$ [14].

In most of the non-diffractive inelastic interactions partons from A and B slow down and combine to produce low momentum hadrons which populate the central region (i.e. the angular region which is transverse to the colliding beam).

Remnants of A and B continue travelling in the forward and backward direction and will eventually recombine into hadrons. The momentum transferred in parton interactions in the central region is usually quite small. In the final state the total transverse momentum (p_t) is only a small fraction of the total momentum (p) of the interacting particles and the collision is said to be “soft”.

Non-diffractive inelastic interactions are those that involve net colour exchange between the two incoming hadrons, while diffractive topologies arise from the exchange of colour neutral objects [14].

Occasionally, two partons pass very close to each other in a non-diffractive interaction. These two partons collide at small impact parameter (b) and are scattered at wide angles. As the impact parameter is the conjugate variable to the transverse momentum, a parton-parton interaction at small impact parameter has a large transverse momentum. Compared to the usual central region processes, these high- p_t scatterings require the transferred momentum to be very high and are therefore called “hard” scattering processes.

Partons scattered at small b , or high- p_t , contain a considerable fraction of the total momentum of the colliding hadrons and thus have enough momentum to attempt to escape the confinement region which leads to the production of jets of hadrons. High- p_t jets therefore stem from the hadronisation of high- p_t scattered partons and are almost back-to-back, with wide angles relative to the hadron’s colliding direction.

In modern high-energy hadron colliders, where the centre of mass energy (\sqrt{s}) is of the order of, or greater than 10 GeV, non-diffractive inelastic interactions are the most common type of hadron scattering. These events will typically result in two jets of fast moving particles containing fragments of A and B roughly in the forward and backward directions, with a central region populated by low momentum particles.

4.1 The Total Collision Cross-Section

In hadron-hadron scatterings, the total collision cross-section, σ_{tot} , can be divided into elastic (σ_{elas}) and inelastic (σ_{inel}) processes. It is also usual to sub-divide inelastic scattering into diffractive (single and double diffraction - σ_{sd} and σ_{dd} , respectively) and non-diffractive processes (σ_{nd}) [14]. Thus, the total cross section, σ_{tot} , is subdivided according to

$$\sigma_{tot}(s) = \sigma_{elas}(s) + \sigma_{sd}(s) + \sigma_{dd}(s) + \sigma_{nd}(s), \quad (5)$$

where s is the square of the total centre of mass energy.

As examples, we show in Figures 3 and 4, respectively, the total and elastic cross sections measured for proton-proton (pp) and proton-anti-proton ($p\bar{p}$) collisions as a function of \sqrt{s} [15]. Most of the data comes from collider experiments, but there are also some points obtained from pp

interactions at very high \sqrt{s} ($\sqrt{s} \gtrsim 10$ TeV) which come from cosmic ray experiments [15].

Figures 3 and 4 indicate that for both pp and $p\bar{p}$ interactions, the total cross-section increases with \sqrt{s} . If this rise is extrapolated to the Large Hadron Collider (LHC) design energy $\sqrt{s} = 14$ TeV with an energy dependence dominated by $\sigma_{tot} \sim \ln^2(s)$ the total cross-section, predicted by the Froissart-Martin theorem [16], is estimated to be $\sigma_{tot} \sim 130$ mb whereas if as $s \rightarrow \infty$, σ_{tot} tends instead to a constant, then $\sigma_{tot} \sim 90$ mb. The expectation for the LHC is thus $\sigma_{tot} \sim 110 \pm 20$ mb [17].

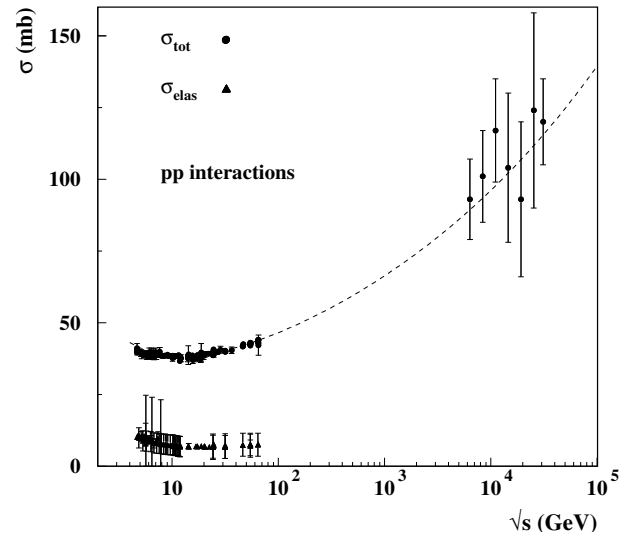


Figure 3: Total and elastic cross-section for pp interactions [15].

At high-energies, elastic events contribute less than inelastic to the total cross-section. At the LHC it is estimated that $\sigma_{inel}/\sigma_{tot} \sim 0.75$ [17]. Among the inelastic events, non-single diffractive are the dominant processes [14].

In the complex environment of inelastic hadronic interactions the separation of soft and hard processes is totally artificial. However, one can look for particular classes of events characterised by a dominant signature of either soft or hard partonic interactions. Signatures typically used for identifying specific hadronic interactions include jets, rapidity gaps, energy and momentum distributions among others. In experimental terms, these event signatures are used to trigger the detection systems and record all relevant information to the study of the underlying physics.

QCD indicates that high- p_t parton scatterings (say $p_t > 2$ GeV/c) are usually rare events, while low- p_t scatterings are the dominant processes in high-energy hadron collisions [8]. Hadronic inelastic interactions are virtually all characterised by low- p_t parton scatterings, although there is also a small probability of having high- p_t processes as part of the inelastic events.

QCD has been fairly successful in describing quark, anti-quark and gluon scatterings involving large amounts of transverse momenta known as “hard” interactions. However high-energy pp and p \bar{p} collisions are dominated by soft partonic collisions, so-called minimum bias events. Soft partonic interactions also occur in the remains of hard scattering events not associated with the hard process and this is important for many physics analyses such as Higgs VBF search [18].

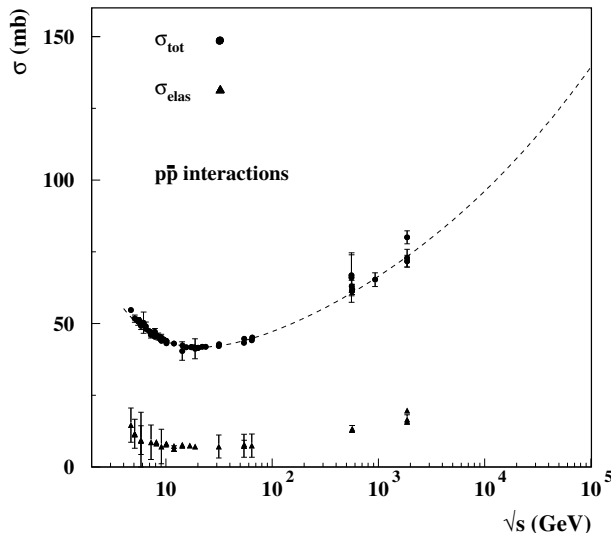


Figure 4: Total and elastic cross-section for p \bar{p} interactions [15].

QCD breaks in the region of soft interactions due to two effects. At $\Lambda_{\text{QCD}} \sim \text{few hundred MeV}$, $\alpha_s \sim 1$ and perturbative QCD breaks down. At momentum transfer of $\sim \text{few GeV}$, the partonic cross-section σ_{QCD} for a $2 \rightarrow 2$ parton scattering will exceed the pp or p \bar{p} cross-section. One method of solving this has been to introduce multiparton interactions for which there is an increasing number of supporting experimental evidence [19–21].

Current models of high-energy hadron collisions will typically combine perturbative QCD to explain parton interac-

tions where it is applicable (high- p_t scatterings), with an alternative phenomenological approach to describe soft processes. Examples of these are the Dual Parton Model (DPM) [22] and modified versions of QCD in which the divergences presented by the running coupling constant are phenomenologically corrected to reproduce experimental observations [23].

4.2 Hadron Scattering Variables

In circular colliders, two stored beams of stable hadrons, A and B, are made to collide head on. If A and B have equal and opposite momenta, their four-momenta are

$$\begin{aligned} p_A &= (E_A, \mathbf{p}) \\ p_B &= (E_B, -\mathbf{p}), \end{aligned} \quad (6)$$

with the square of the total centre-of-mass energy, s , given by

$$s = (E_A + E_B, \mathbf{p} - \mathbf{p})^2 = (E_A + E_B)^2. \quad (7)$$

For particles produced with an angle θ with respect to the beam direction, the longitudinal (p_l) and transverse (p_t) momentum are defined as

$$p_l = |\mathbf{p}| \cos \theta \quad (8)$$

$$p_t = |\mathbf{p}| \sin \theta, \quad (9)$$

respectively. Notice that p_t is invariant under a transformation from the centre-of-mass to the laboratory frame. The fraction of the beam’s momentum \mathbf{p} carried by the longitudinal component p_l of final state particles is defined as

$$x = \frac{p_l}{|\mathbf{p}|}, \quad (10)$$

also known as Feynman’s x and limited to $-1 < x < 1$. Typically in a high-energy hadron collision, most of the particles will be produced with x near 0, and as mentioned before, will populate the central region.

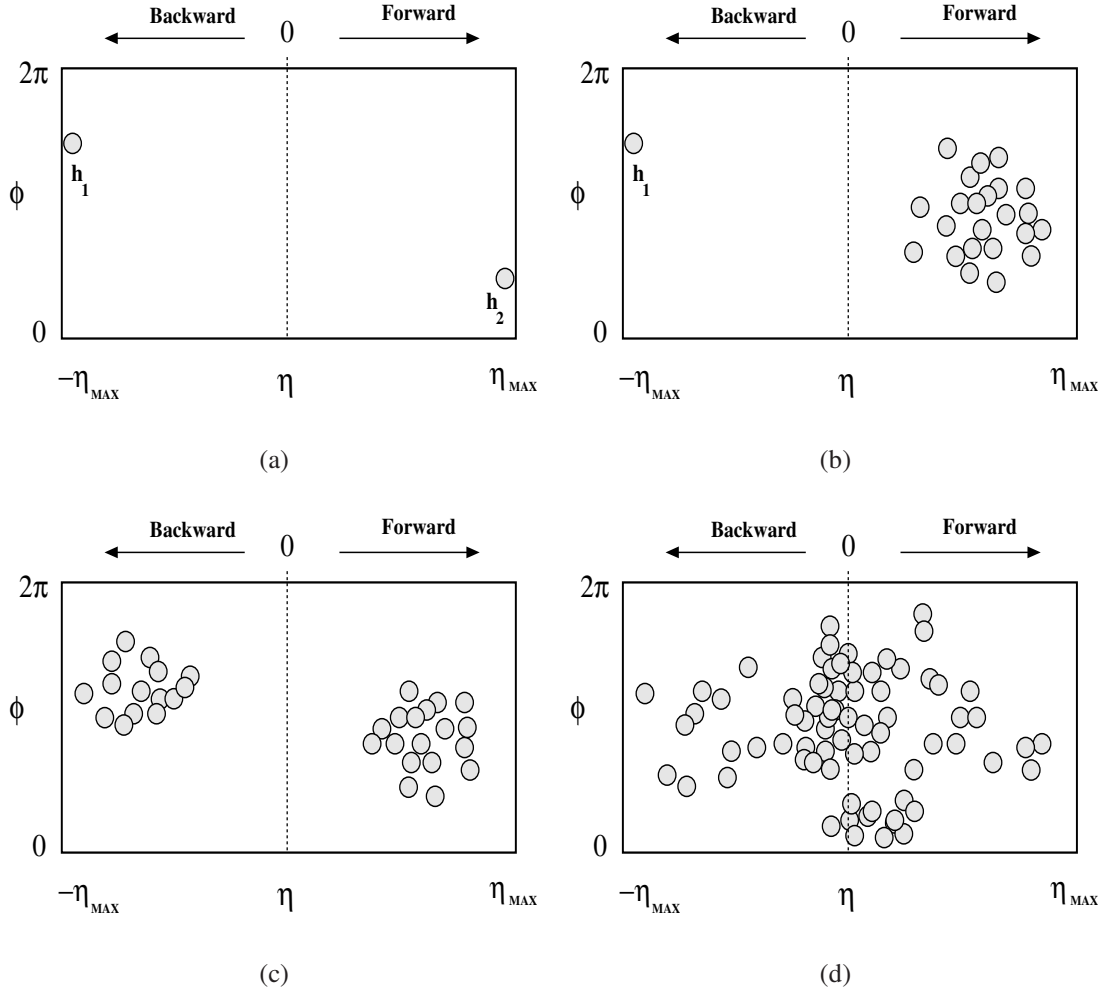


Figure 5: Schematic view of (a) elastic, (b) single-diffractive, (c) double-diffractive and (d) non-diffractive hadron interactions in the $\eta - \phi$ space.

Another longitudinal variable widely used in high-energy hadron collisions is the so-called rapidity (y), defined as

$$y = \frac{1}{2} \ln \left(\frac{E + p_l}{E - p_l} \right). \quad (11)$$

The rapidity gives information on the velocity component of particles along the beam axis. It depends on the choice of frame, but has the advantage that rapidity differences are invariant under Lorentz boosts along the beam direction.

In high-energy processes it is more convenient to use a modification of y which is independent of the mass of the particle. This pseudo-rapidity, η , is written as

$$\eta = \frac{1}{2} \ln \left(\frac{p + p_l}{p - p_l} \right) = -\ln \left(\tan \frac{\theta}{2} \right) \quad (12)$$

and is a good approximation of y as long as the mass is small compared to p_l .

Particles produced in the central region have small values of η and distribute themselves around $\eta = 0$ (corresponding

to $\theta = 90^\circ$, i.e. transverse to the colliding beam), while particles travelling in the forward or backward fragmentation regions have $|\eta|$ greater than a few units of η .

The pseudo-rapidity spectrum of a hadron collision, shows well defined pseudo-rapidity gaps as a signature of diffractive events. These gaps correspond to the separation in pseudo-rapidity between the two jets of particles produced in the forward and backward regions. In the case of a single diffractive interaction, one of the incident particles is scattered quasi-elastically and loses very little of its momentum, emerging from the collision with $|x|$ close to 1. The other initial particle breaks up into a system of hadrons, of invariant mass M ($M^2 \ll s$), which are well separated in rapidity from the first incident particle (or system of hadrons in the case of double diffraction).

Pseudo-rapidity gaps are absent in non-diffractive inelastic processes due to the production of particles in the central region.

Figure 5 shows a schematic view of elastic (a), single-

diffractive (b), double-diffractive (c) and non-diffractive inelastic hadron interactions (d) in the $\eta - \phi$ phase space, the angle ϕ being the azimuthal scattering direction.

As schematically shown in Figure 5(a), the hadron separation in pseudo-rapidity is maximum for elastic scatterings. Single and double diffractive events, shown in Figures 5(b) and (c) respectively, display clear separation, or gaps, between the systems travelling in the forward and backward regions. However, for particles produced in a non-diffractive event, as displayed in 5(d), gaps which naturally occur between two systems moving in opposite directions (forward and backward) are filled by particles produced in the central region.

4.3 Particle Density in Pseudorapidity

The rate of parton-parton scattering in a hadronic collision is strongly correlated to the observed particle multiplicity and the pseudorapidity distribution of produced particles. This happens because multiple parton interactions convert part of the collision energy that would otherwise be carried by the fast moving system of beam-remnants in the forward regions, into low- p_t particles which populate the central region.

Figure 6 displays charged particle densities, $dN_{ch}/d\eta$, distributed in the pseudorapidity space, η , for non-single diffractive inelastic (i.e. non-diffractive inelastic and double-diffractive processes) $p\bar{p}$ collisions at $\sqrt{s} = 200$ GeV [24], 900 GeV [24] and 1.8 TeV [25]. It shows a central plateau at small η and a falling density in the fragmentation region, i.e. $\eta \rightarrow \eta_{max}$.

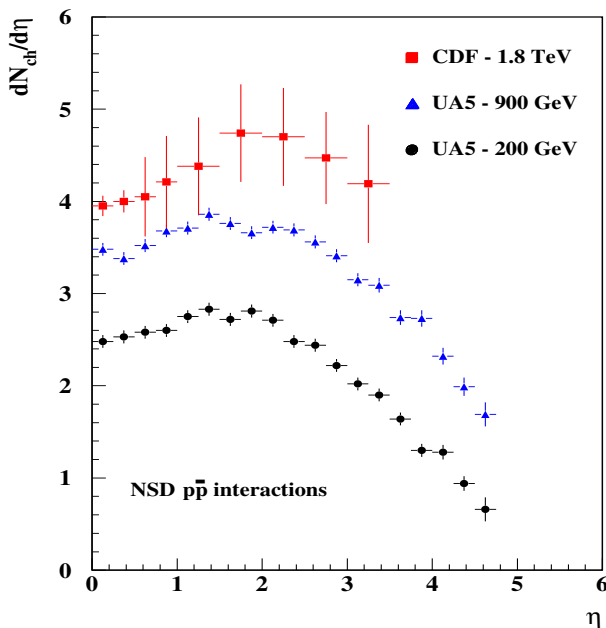


Figure 6: Charged particle density distributions, $dN_{ch}/d\eta$, for non-single diffractive inelastic $p\bar{p}$ collisions at $\sqrt{s} = 200$ GeV [24], 900 GeV [24] and 1.8 TeV [25].

As the colliding energy increases, the rate of multiple parton interactions also increases producing a rise on the central plateau. Therefore, in order to correctly describe $dN_{ch}/d\eta$, one has to correctly reproduce the amount of partonic activity (multiple parton scattering) taking into account the expected variation with the colliding energy.

5 The Large Hadron Collider

Most of our information about the structure and properties of hadrons and their constituent partons is based on the analysis of high-energy scattering data obtained through many experiments performed in the last fifty years. In this context, particle colliders have become indispensable tools to the progress of high-energy physics.

From the experimental point of view, the use of accelerators, both fixed target and collider, has proved to be not only a good source of information but an essential tool in the development of particle physics [1, 2]. Experiments designed to probe kinematic regions not yet explored have the potential to provide crucial information required to advance our knowledge on elementary particles and their interactions. In this context, the field of particle physics will benefit immensely from the observations to be made at the Large Hadron Collider (LHC) which is currently under construction at CERN [26, 27].

The LHC will collide protons at centre-of-mass energies many times greater than any hadron collision ever performed in laboratory. This accelerator follows a series of successful high-energy hadron colliders which started in the 1970's with the CERN's Intersecting Storage Rings (ISR) and evolved to increasingly higher-energy colliders such as the CERN's Super Proton Synchrotron (SPS) during the 1980's and the Fermilab's Tevatron which is still operational.

The LHC is being built in a 27 km circumference tunnel which once accommodated LEP, will collide protons at a centre of mass energy of $\sqrt{s} = 14$ TeV [27]. Besides protons, the LHC will also accelerate and collide beams of lead nuclei at a centre of mass energy of $\sqrt{s} = 1150$ TeV.

The number of particles per square-centimeter per second generated in the beams of high energy particle experiments is called luminosity. The higher the luminosity, the greater the number of events produced for study. For the proton runs, the design luminosity (also referred to as "high luminosity") is $10^{34} \text{ cm}^{-2}\text{s}^{-1}$, but during the first year the LHC will also run at a lower luminosity, namely $2 \times 10^{33} \text{ cm}^{-2}\text{s}^{-1}$ (referred to as "low luminosity").

Besides the large potential to discover new physics, e.g. the Higgs boson and Supersymmetry (SUSY), the LHC will also test the predictive power of the Standard Model for

particle interactions at an energy regime never probed before. This includes precise measurements of electroweak processes and observations of some of the most complicated properties of strong interactions.

At the LHC, essentially all physics processes will be somehow connected to quark and gluon interactions. Thus, high-energy proton collisions at the LHC are expected to reveal aspects of parton interactions which will greatly improve our understanding of QCD for both high and low- p_t processes.

6 Conclusions

Although our knowledge on the partonic structure of hadrons accumulated so far allows successful descriptions of many aspects of particle interactions to be made, uncertainties associated to the breakdown of QCD at low- p_t and to parton densities still remain and limit the accuracy of theoretical predictions. Experiments, such as the LHC, designed to probe kinematic regions not yet explored can provide crucial information to reduce the current level of these uncertainties.

High-energy hadron interactions are the product of interactions between the elementary particles which constitute the interacting hadrons. The LHC and its planned experiments will certainly provide significant new insights on the exciting field of hadron interactions at high-energy. Running at very high centre-of-mass energies, the LHC experiments will test the predictive power of the Standard Model for particle interactions at an extreme energy regime. Due to the LHC's high luminosity, experiments such as ATLAS and CMS [27] will also benefit from large statistical samples of data for many interesting channels. This will considerably reduce the current levels of statistical uncertainties in many precise measurements with the overall precision of measurements being limited by systematics effects.

Performing precise measurements in a large number of physics channels such as jet measurements, direct photon production, Drell-Yan processes and heavy flavour production, in most cases, the LHC experiments are expected to improve significantly on previous experiments. These measurements will lead to remarkable improvements in our knowledge of hadron interactions.

References

- [1] R. N. Cahn and G. Goldhaber, *The Experimental Foundations of Particle Physics*, Cambridge, 1989.
- [2] F. Close, M. Marten and C. Sutton, *The Particle Odyssey: A Journey to the Heart of the Matter*, Oxford, 2002.
- [3] E. Rutherford, *Phil. Mag.* **21** (1911) 669.
- [4] J. Chadwick, *Nature* **129** (1932) 312.
- [5] C. D. Anderson, *Phys. Rev.* **43** (1933) 491.
- [6] S. H. Neddermeyer and C. D. Anderson, *Phys. Rev.* **51** (1937) 884;
J. C. Street and E. C. Stevenson, *Phys. Rev.* **52** (1937) 1002.
- [7] C. M. G. Lattes *et al.*, *Nature* **159** (1947) 694;
C. M. G. Lattes, G. P. S. Occhialini and C. F. Powell, *Nature* **160** (1947) 453.
- [8] P. D. B. Collins and A. D. Martin, *Hadron Interactions* (Graduate student series in physics), Adam Hilger, Bristol, 1984.
- [9] M. Gell-Mann, *Phys. Lett.* **8** (1964) 214.
- [10] F. Abe *et al.*, *Phys. Rev. D* **50** (1994) 2966;
F. Abe *et al.*, *Phys. Rev. Lett.* **73** (1994) 225;
S. Abachi *et al.*, *Phys. Rev. Lett.* **72** (1994) 2138.
- [11] M. E. Peskin and D. V. Schroeder, *An Introduction to Quantum Field Theory*, Perseus Books, 1995;
F. Mandl and G. Shaw, *Quantum Field Theory*, Wiley, 1993;
F. Halzen and A. Martin, *Quarks and Leptons: An Introductory Course in Modern Particle Physics*, Wiley, 1984.
- [12] G. Arnison *et al.* (UA1 Collaboration), *Phys. Lett. B* **122** (1983) 103;
M. Banner *et al.* (UA2 Collaboration), *Phys. Lett. B* **122** (1983) 476.
- [13] G. Arnison *et al.* (UA1 Collaboration), *Phys. Lett. B* **126** (1983) 398;
P. Bagnaia *et al.* (UA2 Collaboration), *Phys. Lett. B* **129** (1983) 130.
- [14] G. A. Schuler and T. Sjöstrand, *Phys. Rev. D* **49**(5) (1994) 2257.
- [15] K. Hagiwara *et al.*, *Phys. Rev. D* **66**, 010001 (2002).
- [16] J. R. Forshaw and D. A. Ross, *Quantum Chromodynamics and Pomeron*, Cambridge (1997).
- [17] D. Denegri, *Standard Model Physics at LHC (pp collisions)*, In: J. Göran and R. Dieter (eds.) ECFA - Large Hadron Collider Workshop, p.57-116. Aachen, October 1990.
- [18] S. Asai *et al.* *Eur. Phys. J., C* **32S2** (2004) 19.
- [19] T. Akesson *et al.*, *Z. Phys. C* **34** (1987) 163.
- [20] J. Alitti *et al.*, *Phys. Lett. B* **268** (1991) 145.

- [21] F. Abe *et al.*, Phys. Rev. D **47** (1993) 4857;
F. Abe *et al.*, Phys. Rev. Lett. **79** (1997) 584;
F. Abe *et al.*, Phys. Rev. D **56** (1997) 3811.
- [22] A. Capella *et al.* Phys. Lett. **81B**(1) (1979) 68;
A. Capella and J. T. T. Van, Phys. Lett. **93B**(1,2) (1980)
146;
A. Capella and J. T. T. Van, Z. Phys. C **10** (1981) 249;
A. Capella *et al.*, Phys. Rep. **236**(4,5) (1994) 225.
- [23] T. Sjöstrand and M. van Zijl, Phys. Rev. D **36**(7) (1987)
2019.
- [24] R. E. Ansorge *et al.*, Z. Phys. C **43** (1989) 357.
- [25] F. Abe *et al.*, Phys. Rev. D **41**(7) (1990) 2330.
- [26] The European Organization for Nuclear
Research - CERN. Public web-pages at:
<http://public.web.cern.ch/public/>.
- [27] The Large Hadron Collider, Conceptual Design,
CERN-AC-95-05 LHC, October 1995.